Astron. Astrophys. 354, 280–286 (2000)

ASTRONOMY AND ASTROPHYSICS

The influence of the solar atmospheric stratification on the form of p-mode ridges

S. Steffens and F. Schmitz

Astronomisches Institut der Universität Würzburg, Am Hubland, 97074 Würzburg, Germany

Received 11 August 1999 / Accepted 9 November 1999

Abstract. We investigate properties of non-radial solar p-modes of high angular degree. We consider linear adiabatic oscillations with the transition layer as an ideal reflector. Ionization of hydrogen and helium and dissociation of hydrogen are included in the equation of state and consequently in the adiabatic sound speed. Because of the restriction to high-degree modes we use the plane layer approximation with constant gravity. Our standard atmospheric model is the VAL-C atmosphere. This atmosphere is joined to the upper part of a convection zone. A model corona is matched to the transition region. Boundary conditions are applied at the temperature maximum of the corona and at a depth in the convection zone far below the lower turning point of the non-radial p-modes determined by the Lamb-frequency. We vary the temperature stratification of the atmosphere and shift the position of the transition region to obtain a family of eight different equilibrium models. By this strategy we can study the formation of structures in the diagnostic diagram and we can take into account uncertainties of the VAL-chromosphere. It is shown how the classical p-modes of a convection zone with zero pressure boundary condition are deformed when the thickness of the overlying atmosphere is enlarged. In no case, the atmosphere generates additional modes. By strong bending, horizontally passing parts of the ridges are formed. These parts produce more or less pronounced chromospheric ridges or features. These chromospheric ridges appear at frequencies where observations show enhanced power in the diagnostic diagram. Their locations sensitively depend on the atmospheric model. A simple two layer model shows that the occurence of bending of the ridges in the diagnostic diagram is quite natural and independent of atmospheric details.

Key words: waves – Sun: atmosphere – Sun: chromosphere – Sun: oscillations

1. Introduction

Investigations of the behavior of non-radial solar oscillations with large horizontal wave numbers ($l \approx 1000 - 2000$) are important with regard to the knowledge of the structure and the dynamics of the atmospheric layers of the sun. In the observational diagnostic diagram, i.e. in the ν–l-plane, non-radial modes appear as broadened ridges.

The ridges extend far beyond the acoustic cut-off frequency of the chromosphere (Libbrecht 1988, Steffens et al. 1995, and Jefferies 1998). Whereas the ridges below the cut-off frequency are commonly attributed to real modes, the nature of the ridges above the cut-off frequency is controversial.

Some observations support the assumption that ridges above the cut-off frequency represent real modes which are caused by reflections of waves at the chromospheric-coronal transition layer. Stebbins & Goode (1987) and Fleck & Deubner (1989) report on the discovery of downward propagating waves. The analysis of data indicates a field of standing waves between the convection zone and the upper chromosphere (Fleck & Deubner 1989). A review of this subject is given by Deubner (1998). An extensive discussion of the acoustic cavity which results from a reflecting transition layer is given by Balmforth & Gough (1990). Recently, Gouttebroze et al. (1999) have concluded from observations of UV-lines that waves are entirely reflected by the transition layer.

For $l \gg 1$, the approach of modeling the outer layers of the sun by a plane layer with constant gravity is common. In this case, the discrete number l is replaced by a continuous horizontal wave number k. Papers investigating the behavior of high-degree p -modes with a plane layer approximation are quoted by Schmitz & Steffens (1999).

The reflectivity of the transition layer, however, is controversial. Two interpretations of the high-frequency ridges assume that there are no significant wave reflections at the coronal transition layer, a property attributed to temporal and spatial variations of this layer. Kumar et al. (1990) and Kumar & Lu (1991) have shown that constructive interferences of running waves can generate ridges above the cut-off frequency. Further, solutions of the adiabatic wave equation with discrete complex frequencies which represent outwards travelling, time-damped waves also lead to ridges above the acoustic cut-off frequency. Investigations of such solutions of the adiabatic wave equation have been performed by Hindman & Zweibel (1994).

In the present paper, we do not try to answer the question which effect causes ridges above the critical frequency. We investigate the behavior of modes under the assumption that the

Send offprint requests to: schmitz@astro.uni-wuerzburg.de

transition layer is an ideal reflector. Above all, we study the influence of the chromospheric temperature stratification on the form of the ridges. For this purpose we modify the temperature profile of the VAL-model and change the position of the reflecting transition layer. Further, we study the occurence of so-called chromospheric modes and the question of the formation of new ridges by the existence of the atmosphere. We consider only adiabatic waves, but include ionization and dissociation in the equation of state.

In Sect. 2 we present the wave equations and explain the method of integrating the wave equations and the atmospheric equilibrium models. In Sect. 3 details of the different models are presented. Sect. 4 deals with the modes, their classification, and the behavior and the form of the ridges. The ridges of the modes of a simple two-layer model are presented in Sect. 5 in order to show that the bending is a basic natural effect. In Sect. 6 we briefly point to coincidences with observational results.

2. The wave equations and the static atmosphere

Let z be the vertical, outwards directed geometrical coordinate, g the constant gravity, ρ the density, $p = p_g + p_t$ the total pressure, p_g the gas pressure, p_t the turbulent pressure of the chromosphere, and c the adiabatic sound speed. The horizontal cartesian coordinates x and y, and the time t are separated by $\exp[\,i\,(\omega\,t - k_x\,x - k_y\,y)]$, where ω is the real frequency, and k_x and k_y are the horizontal wave numbers. From the linearized hydrodynamic equations we obtain two first order differential equations (cf. e.g. Schmitz & Fleck 1994)

$$\frac{d}{dz}\,\xi - g\,\frac{k^2}{\omega^2}\,\xi = -\frac{1}{\omega^2\,\rho c^2}\,(\omega^2 - c^2k^2)\,\Delta p\;, \tag{1}$$

$$\xi = -\left[\,\frac{k^2g^2}{\omega^2} - \omega^2\,\right]^{-1}\frac{1}{\rho}\,(\frac{d}{dz}\,\Delta p + g\,\frac{k^2}{\omega^2}\,\Delta p)\;. \tag{2}$$

Here, ξ is the vertical displacement, Δp the total Lagrangian pressure perturbation, and $k^2 = k_x^2 + k_y^2$.

By the transformation $\xi = p^{-1/2}\,\zeta$, $\Delta p = p^{+1/2}\,\eta$ we obtain a system which is more suitable for a numerical integration:

$$\frac{d}{dz}\zeta = g\,\left[\,\frac{k^2}{\omega^2} - \frac{1}{2}\frac{\rho}{p}\,\right]\,\zeta - \frac{1}{\omega^2}\,(\omega^2 - c^2k^2)\,\frac{p}{\rho\,c^2}\,\eta\;, \tag{3}$$

$$\frac{d}{dz}\eta = -\,g\,\left[\,\frac{k^2}{\omega^2} - \frac{1}{2}\frac{\rho}{p}\,\right]\,\eta - \left[\,\frac{k^2g^2}{\omega^2} - \omega^2\,\right]\,\frac{\rho}{p}\,\zeta\;. \tag{4}$$

For an isothermal atmosphere with the equation of state of the classical ideal gas, this system has constant coefficients.

The VAL-C model atmosphere is smoothly matched to the convection zone of Spruit (1977) and to the corona of Dupree (1972). We cut the corona at its temperature maximum, where we apply the upper boundary conditions assuming an overlying isothermal atmosphere with infinite extension. The thermodynamic state of the gas is described by an LTE equation of state with dissociation and ionization of hydrogen and helium (H_2, H, H^+, He, He^+, He^{++}, e^-). The density $\rho(p_g, T)$ and the adiabatic sound speed $c(p_g, T)$ are calculated with a code developed by Wolf (1983). From the published thermodynamic quantities of the convection zone, the VAL-atmosphere, and the corona, we take only the temperature $T(z)$. Besides, we use the turbulent pressure $p_t(z)$ of the VAL-C-Model. This pressure has been introduced to account for the observed line spectrum. The used model of the convection zone do not contain a turbulent pressure. We integrate the equilibrium equation

$$\frac{d}{dz}\,p(z) = -\,g\,\rho(p_g(z), T(z)) \tag{5}$$

at equidistant mesh points z_i by the trapezoidal rule to obtain the total equilibrium pressure $p(z_i)$. At the bottom of the layer, the temperature is $T = 7.\,10^5$ K. The top of the layer is at the position of the temperature maximum $T = 1.563\,10^6$ K of the corona. The thickness of the total layer is $2.687\;10^4$ km. The step width is $\Delta z = 1$ km.

For the numerical integration of the wave equations we use the explicit extrapolation integrator of Deuflhard (1980). Here, the method of weighted parabolas (Kurucz 1973) is used to interpolate the thermodynamic quantities $\rho(z)$, $p(z)$, and $c(z)$ from their discrete values ρ_i, p_i, and c_i given at the equally spaced mesh points z_i. At the top of the layer we use the analytic solution of evanescent waves of an isothermal atmosphere to obtain an upper boundary condition. In general, the results do not change significantly when we replace this boundary condition by the condition $\Delta p = 0$ at the position of the coronal transition layer.

3. Variations of the standard model

We intend to study the influence of the atmospheric layers on the form of the p-mode ridges. Therefore, as in the paper of Steffens et al. (1997) we use the following model atmospheres:

I. The VAL-C atmosphere: The model C of Vernazza et al. (1981) is our standard model.

II. A cold chromosphere: Here, the temperature is constant from the position of the VAL-temperature minimum to the position of the transition layer. A variant of this configuration is obtained by enlarging the extension of the isothermal chromosphere by 500 km. This model was selected with reference to the cold chromosphere of Carlsson & Stein (1995, 1998). The enlarged extension of the cold chromosphere is used to study the influence of variations of the position of the transition layer on the form of the p-mode ridges.

III. An isothermal atmosphere: Here, an isothermal layer with a temperature equal to the mean temperature of the VAL-chromosphere is matched to a convection zone with a smoothed photosphere. We obtain three additional variants of this model by reducing the position of the transition layer by 400, 800, and 1400 km. In addition, we use the pure convection zone without the overlying isothermal atmosphere. These models are used to study the behavior of the ridges with regard to the position of the transition layer.

The standard model and some of its variations are shown in Fig. 1.

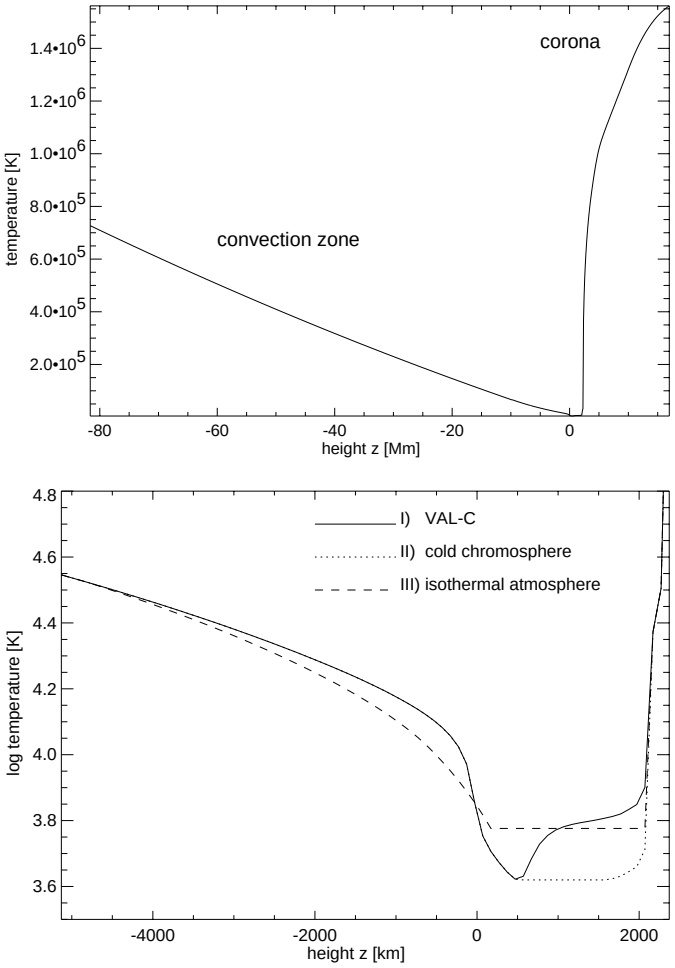

Fig. 1. The temperature profile T(z) and a magnification of the photospheric and chromospheric regions

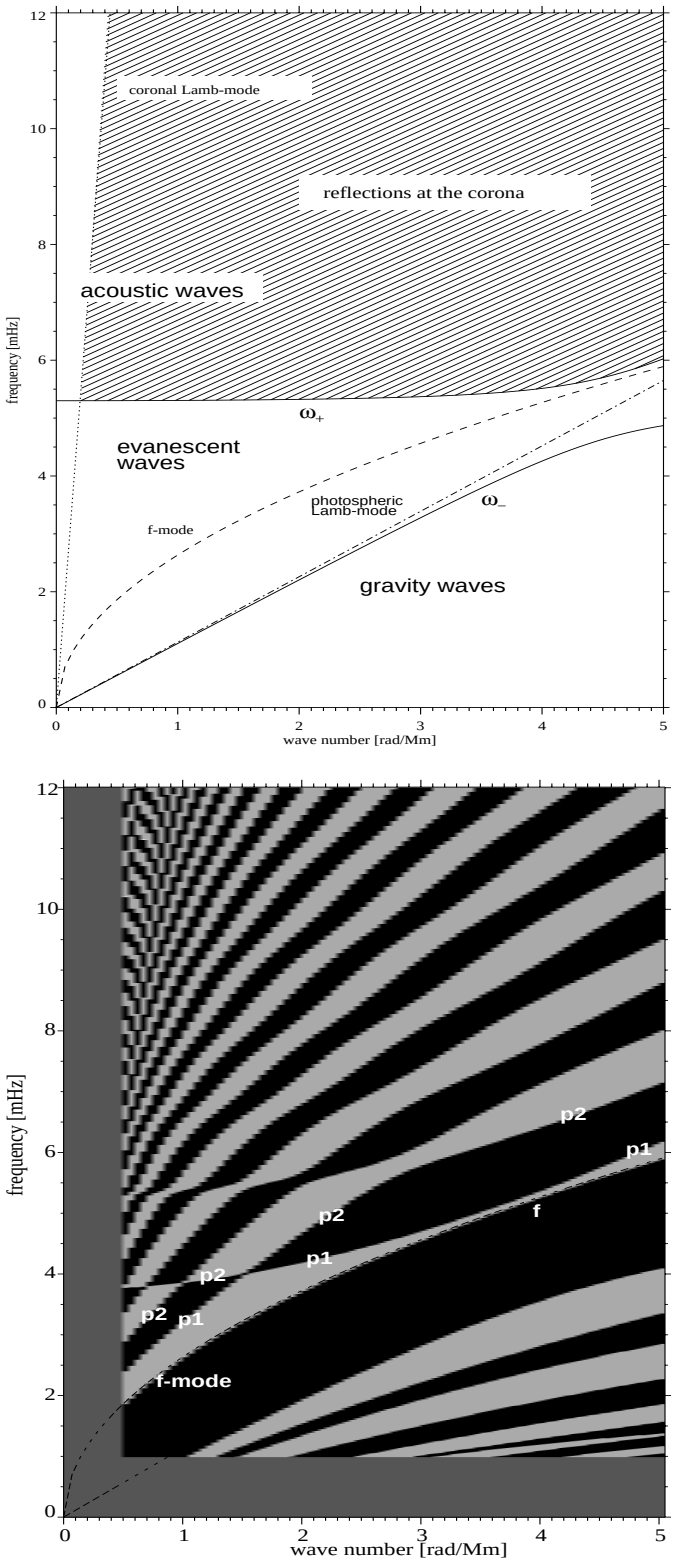

Fig. 2. Diagnostic (k, ν-) diagrams for isothermal layers (photosphere and corona) and for the standard model. In the case of the isothermal layers, the frequencies ω_+ and ω_- are the critical frequencies of the photosphere. For the standard model, divergent solutions of the wave equation are represented by black or grey areas depending on the sign of the diverging amplitudes. The boundary lines of the areas are the ridges, where the solutions "converge".

4. The modes and their ridges

We integrate the wave equations from the position of the temperature maximum of the corona downwards to the bottom of the convection zone. Below the lower turning point z_L of the non-radial p-modes in the convection zone given by $\omega = c(z_L)\, k$, the solution is non-oscillatory and evanescent. We calculate the eigenfunctions and eigenfrequencies by trial and error integrations. The amplitude of the displacement blows up exponentially below the Lamb-level when ω is not close to an eigenvalue ω_n. As in the case of a strict natural boundary condition at a singularity, the displacement starts to diverge when $\omega > \omega_n$ or $\omega < \omega_n$. Because of the finite extension of our convection zone we cannot determine sharp eigenfrequencies. In the case of a natural boundary condition like the vanishing of the displacement at the center of the sun, the eigenvalues are sharp.

4.1. Classification of the p-modes

Strictly speaking, a mode corresponds to a point (k, ω) of the diagnostic diagram. In general, however, the terms p-mode or p-mode-ridge are used synonymously. In the following, we char-

acterize a ridge (or a mode) $\omega(k)$ as the set of all single modes (ω, k) with the same number of radial nodes. The order n of a mode is equal to the number of radial nodes of the Lagrangian displacement $\xi(z)$. In the case of the Cowling approximation, such a classification is possible. Fig. 2. shows p-mode ridges of the standard model.

In the literature, the term chromospheric mode is common. When the atmosphere or the chromosphere are considered as separate, independent systems with corresponding boundary conditions — such layers were studied e.g. by Bahng & Schwarzschild (1963) and McKenzie (1971) — this term is evident.

Besides, the term chromospheric mode is used when global oscillations of the sun or of the outer layers of the sun are studied. Ando & Osaki (1977) and Ulrich & Rhodes (1977) find chromospheric modes, although global oscillations are considered. These authors, however, have studied modes with frequencies below the acoustic cut-off frequency of the chromosphere and with values for the degree l lower than considered in this paper. Besides, Ulrich & Rhodes (1977) have not classified the modes according to the number of radial nodes.

4.2. Discussion of the p-mode ridges

Figs. 3 and 4 show ridges $\nu(k)$ of modes. Besides p-modes, the calculations yield also g-modes. We do not consider g-modes in this paper. Figs. 3c,d and Fig. 4h show results for the restricted frequency range 3 mHz $< \nu <$ 5 mHz, which is sufficient for the purpose of comparison.

Fig. 3a shows the ridges of a pure convection zone without an overlying atmosphere. Here, the boundary condition is $\Delta p = 0$ at the top of the convection zone. Essentially, these ridges behave as the ridges of a polytropic convection zone with isentropic stratification, where $\omega^2 = g\,k\,[1+2(\gamma-1)\,n]$ with $n = 1, 2, ...$ and an adiabatic exponent γ (cf. Lamb 1932).

Then, an isothermal atmosphere with a certain height H is matched to the convection zone (Figs. 3b–d and Fig. 4e). For $H = 600$ km (model b), there are no significant changes of the form of the ridges. The models c, d, and e show ridges of configurations with atmospheric heights $H = 1200, 1600,$ and 2000 km. With increasing height of the atmosphere, the bending of the ridges becomes stronger and is shifted to lower frequencies. In the case of model e, the temperature profile $T(z)$ of which is shown in Fig. 1, the ridges generate an chromospheric feature at 4 mHz. Fig. 4f shows the ridges of the modes of the standard-model. Here, the horizontal branches of the ridges are more pronounced than the corresponding parts of the ridges of the model with the isothermal atmosphere (Fig. 4e). They form a chromospheric feature. There is also a strong bending of the ridges at $\nu \approx 5.3$ mHz. This bending is not present in the case of the model with the isothermal chromosphere (Fig. 4e). In the case of the model with the cool chromosphere (Fig. 4g), the bending of the ridges is shifted to higher frequencies. Also in this case an chromospheric ridge seems to form. When the cool chromosphere is enlarged by 500 km (Fig. 4h), a second strong bending appears so that a second chromospheric ridge seems to exist. Besides, the horizontal branches of the ridges are shifted to lower frequencies. In the cases (f–h) the p_1-mode ridge approaches the atmospheric f-mode at higher wavenumbers k. The results show that the location of a ridge depends on details of the chromospheric structure.

Characterizing the order of a ridge by the number of radial nodes of a mode we find:

New ridges are not formed when an atmosphere is matched to the convection zone. The chromospheric ridges are not separate ridges, but parts of p-mode-ridges of the total layer. Sometimes, these parts look like new, separate ridges. For these horizontal parts, the amplitudes of the modes are large in the chromosphere. A similar behavior is described and displayed by Christensen-Dalsgaard & Frandsen (1983, Fig. 4) for the amplitude of a radial chromospheric mode.

It is difficult to understand details of the structure of the ridges as we have included ionization and dissociation. In this case, the adiabatic sound speed, an important coefficient of the wave equations shows strong variations in the chromosphere (cf. Schmitz & Fleck 1998, Fig. 3). These variations produce reflections of p-modes (e.g. Balmforth & Gough 1990).

5. A two-layer model

In the following, we show that the effect of the bending of ridges already occurs in the case of a simple two-layer configuration without gravity. The layers are isothermal and infinitely extended with respect to the horizontal directions. Let c_1, h_1, and Δp_1 be the sound speed, the thickness and the pressure perturbation of the lower layer, c_2, h_2, and Δp_2 those of the upper layer. In the following example we put $c_1 = 140$ km/s and $c_2 = 7$ km/s, $h_1 = 10.769$ Mm and $h_2 = 0.269$ Mm. The lower layer represents the convection zone, the upper layer the atmosphere. At the bottom $z = 0$ and at the top $z = h_1 + h_2$ of the total layer we put $\Delta p = 0$.

The dispersion relations of the separate layers with zero pressure boundary conditions are

$$\omega = c\sqrt{k^2 + \left(\frac{n\cdot\pi}{h}\right)^2}, \quad \text{with} \quad n = 1, 2, 3, ... \tag{6}$$

where k is the horizontal wave number and $h = h_1$, $c = c_1$ or $h = h_2$, $c = c_2$. The correspondig modes are shown in Fig. 5 by dashed curves.

The conditions for continuity at the interface $z = h_1$ of the combined layers are

$$\Delta p_1 = \Delta p_2 \quad \text{and} \quad c_1^2\,\frac{d}{dz}\,\Delta p_1 = c_2^2\,\frac{d}{dz}\,\Delta p_2\ . \tag{7}$$

The second equation results from the condition for continuity of the vertical displacement. The pressure perturbations are

$$\Delta p_1 = \sin(\kappa_1\, z) \text{ for } 0 \le z \le h_1$$

and

$$\Delta p_2 = A\,\sin(\kappa_2\,(z - (h_1 + h_2)) \text{ for } h_1 \le z \le h_1 + h_2\ , \tag{8}$$

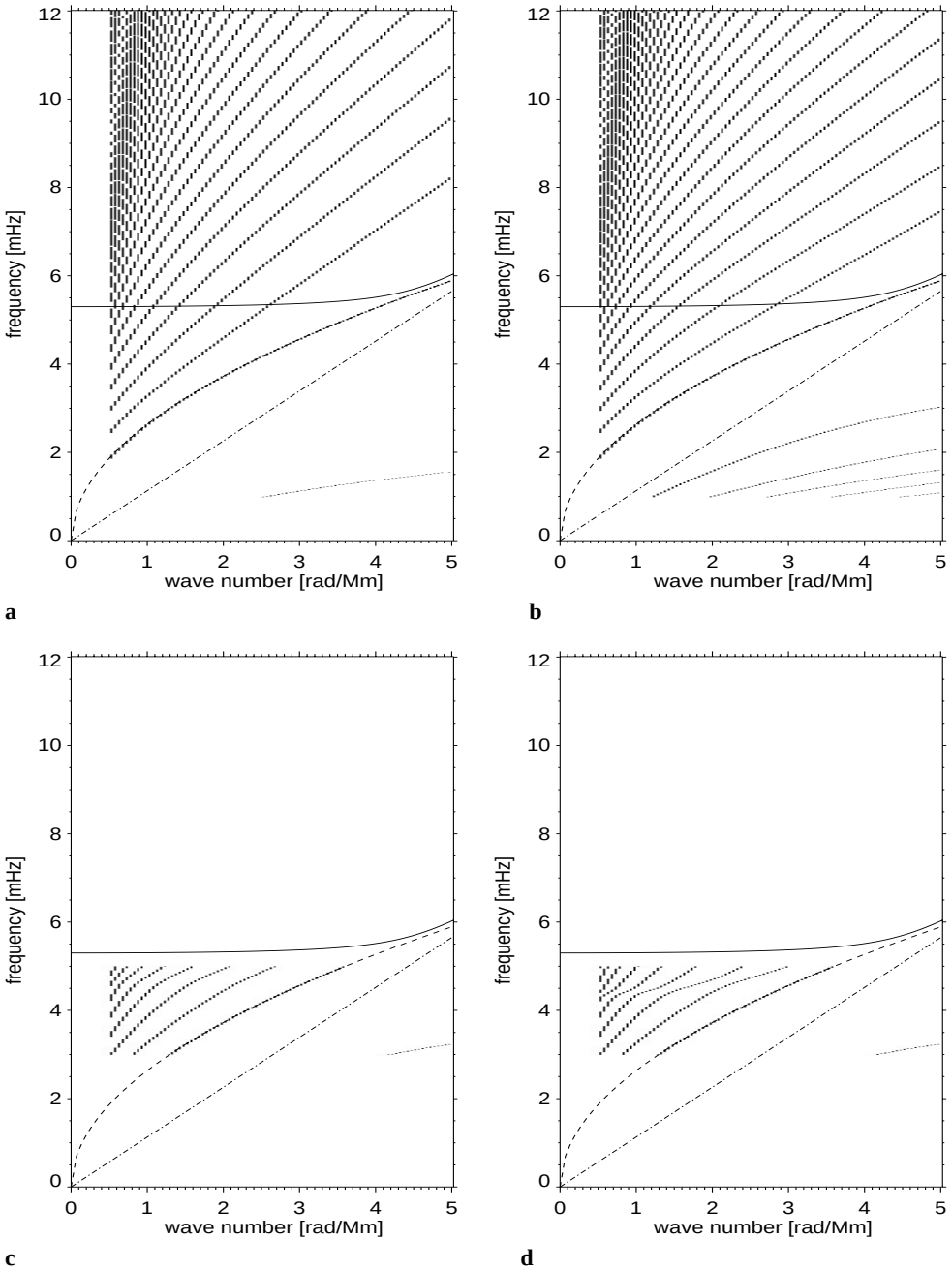

Fig. 3a–d p-mode ridges of the models **a–d**. Model **a** is a pure convection zone without an overlying atmosphere. Models **b–d** are convection zones with isothermal atmospheres. The extension of the atmosphere is 600 km for model **b**, 1200 km for model **c**, and 1600 km for model **d**.

with vertical wave numbers $\kappa_1 = \sqrt{(\omega/c_1)^2 - k^2}$ and $\kappa_2 = \sqrt{(\omega/c_2)^2 - k^2}$. From the conditions for continuity we obtain the dispersion relation

$$\tan[\ \frac{h_1}{c_1}\sqrt{\omega^2 - (c_1 k)^2}\ ] =$$

$$\frac{c_1}{c_2}\sqrt{\frac{\omega^2 - (c_1 k)^2}{\omega^2 - (c_2 k)^2}}\ \tan[\ \frac{h_2}{c_2}\sqrt{\omega^2 - (c_2 k)^2}\ ]\ . \qquad (9)$$

After simplifying this equation by use of dimensionless variables, we have solved it numerically for $\omega > c_1\, k$. The solutions $\nu(k)$ are shown in Fig. 5. (The varying thickness and structure of the lines is due to the numerical result, a set of disarranged and nonuniform $k - \omega$-pairs.) The ridges of the combined layers pass through the intersection points of the ridges of the single layers. One can understand and explain the behavior of the ridges of the total layer by studying the form of the pressure perturbation $\Delta p(z)$. A detailed discussion is given by Steffens (1998). The bending of the ridges at the intersection points can be contributed to the effect of avoided crossing. This effect is extensively described by Christensen-Dalsgaard (1980) for non-radial adiabatic modes of polytropic stellar models and a solar model. Also Hindman & Zweibel (1994) have discussed avoided crossings of modes in the case of a simple model of the outer layers of the sun. Recently, avoided crossings have been found by Gondek & Zdunik (1999) in the behavior of the frequencies of radial pulsations of neutron stars.

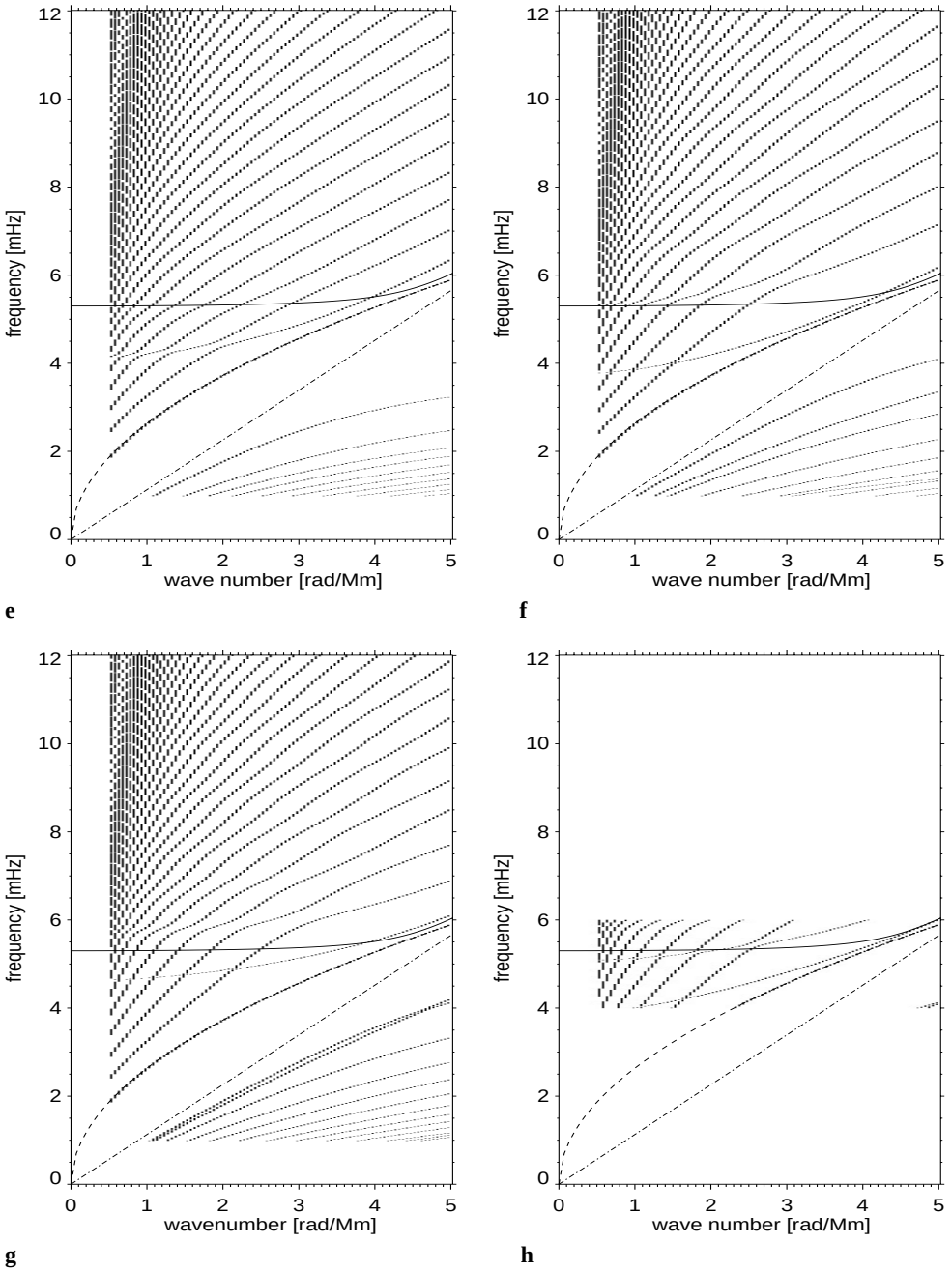

Fig. 4e–h p-mode ridges of the models **e–h**. Model **e** is a convection zone with an isothermal atmosphere the extension of which is 2000 km. Model **f** is the standard model with the VAL-C atmosphere. The chromospheres of model **g** and model **h** are cool, the position of the transition layer of model **h** is shifted by 500 km.

6. Comparison with observational results

Observations by Harvey et al. (1993, 1998) show the presence of a background signal in the powerspectra of p-modes. The frequencies of the signals found by Harvey et al. (1993, 1998) are at $\nu \approx 3.5$ mHz, 5 mHz and 7 mHz. They correspond well to the frequencies of the chromospheric features of our standard model (Fig. 4f). Spatial and temporal variations of the chromosphere and the transition layer can broaden this parts of the modes to a large amount, particularly as we have seen that the postion of the transition layer effects the location of the modes essentially. The arrrangement of the horizontal branches of the ridges in the k, ν-plane also corresponds to the position of the power signal in the background of Na D_2 resolved by Steffens et al. (1995) and to the phase-jumps of this line analysed by Deubner et al. (1996).

7. Conclusions

We have assumed that the whole atmosphere of the sun forms a static cavity, i.e. that the chromospheric-coronal transition layer is quiet and homogenous. We have studied the response of high-degree non-radial p-modes to changes of the atmospheric structure. By varying the chromospheric temperature and the position of the transition layer we find: The global form of the p-mode ridges depends strongly on the thickness of the model atmosphere. In the case of the VAL-C atmosphere the ridges show strong bending. There are nearly horizontal parts of the ridges

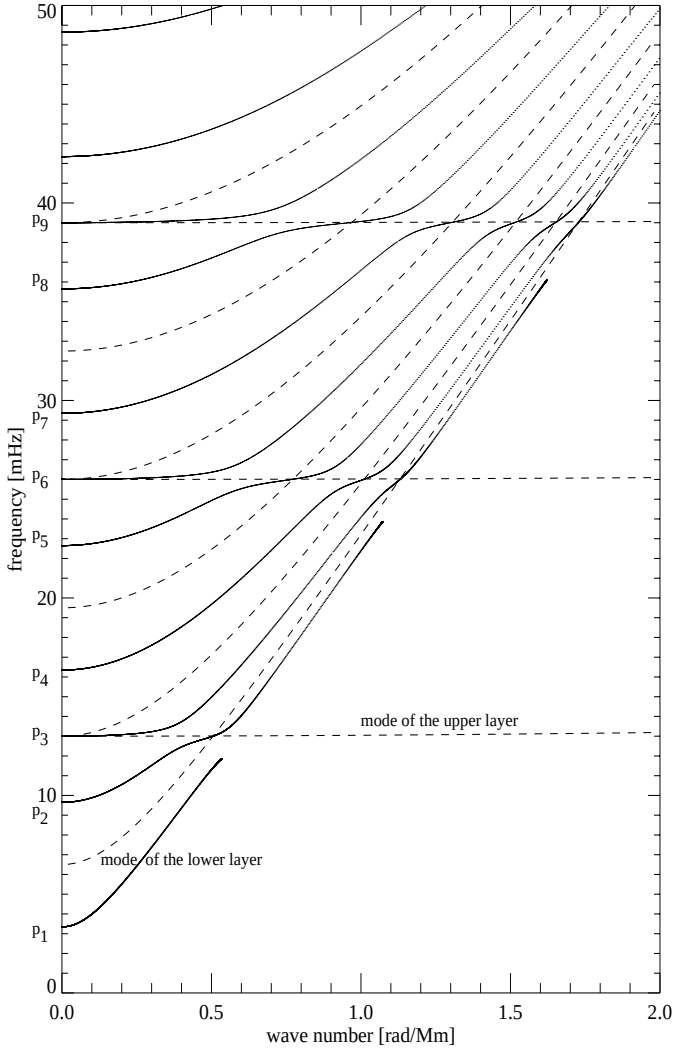

Fig. 5. Modes of a configuration consisting of two isothermal layers (solid or dotted curves). The nearly horizontal modes of the upper layer and the modes of the lower layer are represented by dashed lines.

which join to horizontal features. In the cases of the standard-model and the cool chromosphere it appears that there is an independent chromospheric ridge crossing the p-modes ridges. Strictly speaking, however, besides the p-modes, we find no additional modes.

For the standard-model and the cool chromosphere, the location of the chromospheric ridge and of corresponding features at higher frequencies depends on details of the atmospheric structure. Some observational findings point to the existence of such chromospheric ridges or features. It is also worthy to note that the p_1-mode approaches the atmospheric f-mode at higher values of k.

The sensitive dependence of the location of the chromospheric ridges on variations of the atmospheric structure suggests that physical effects not included in our calculations might be important. Above all, the inclusion of radiative damping of the waves should have some influence on the form of the ridges. Christensen-Dalsgaard (1981) has shown that non-adiabatic effects have significant influence on avoided crossings of non-radial stellar oscillations.

Acknowledgements. S. Steffens gratefully acknowledged the financial support by the Deutsche Forschungsgemeinschaft under grant De 226/11-2.

References

Ando H., Osaki Y., 1977, PASJ 29, 221
Bahng J., Schwarzschild M., 1963, ApJ 137, 901
Balmforth N.J., Gough D.O., 1990, ApJ 362, 256
Carlsson M., Stein R., 1995, ApJ 440, L29
Carlsson M., Stein R., 1998, In: Deubner F.-L., Christensen-Dalsgaard J., Kurtz D. (eds.) IAU Symposium 185, New Eyes to See Inside The Sun and Stars. p. 435
Christensen-Dalsgaard J., 1980, MNRAS 190, 765
Christensen-Dalsgaard J., 1981, MNRAS 194, 229
Christensen-Dalsgaard J., Frandsen S., 1983, Solar Phys. 82, 165
Deubner F.-L., 1998, In: Deubner F.-L., Christensen-Dalsgaard J., Kurtz D. (eds.) IAU Symposium 185, New Eyes to See Inside The Sun and Stars. p. 427
Deubner F.-L., Waldschik T., Steffens S., 1996, A&A 307, 936
Deuflhard P., 1980, Order and Stepsize Control in Extrapolation Methods. SFB 123: Tech. Rep. 93, Universität Heidelberg
Dupree A., 1972, ApJ 178, 527
Fleck B., Deubner F.-L., 1989, A&A 224, 245
Gondek D., Zdunik J.L., 1999, A&A 344, 117
Gouttebroze P., Vial J.C., Bocchialini K., Lemaire P., Leibacher J.W., 1999, Solar Phys. 184, 253
Harvey J., Duvall T.J., Jefferies S., Pomerantz M., 1993, In: Brown T. (ed.) GONG 1992, Seismic Investigations of the Sun and Stars. ASP Conf. Ser. Vol. 42, p. 111
Harvey J., Jefferies S., Duvall T.J., Osaki Y., Shibahashi H., 1998, In: Provost J., Schmider F.X. (eds.) IAU Symposium 181, Sounding Solar and Stellar Interiors. Vol. 2, in press
Hindman B.W., Zweibel E.G., 1994, ApJ 436, 929
Jefferies S., 1998, In: Deubner F.-L., Christensen-Dalsgaard J., Kurtz D. (eds.) IAU Symposium 185, New Eyes to See Inside The Sun and Stars. p. 415
Kumar P., Duvall T.L. Jr., Harvey J.W., et al., 1990, In: Osaki Y., Shibahashi H. (eds.) Lectures Notes in Physics, Progress of Seismology of the Sun and Stars. Springer, Heidelberg, p. 87
Kumar P., Lu. E., 1991, ApJ 375, L35
Kurucz R., 1973, SAO Spec. Rep. 309
Lamb H., 1932, Hydrodynamics. Cambridge University Press
Libbrecht K., 1988, ApJ 334, 510
McKenzie J., 1971, A&A 15, 450
Schmitz F., Fleck B., 1994, A&AS 106, 129
Schmitz F., Fleck B., 1998, A&A 337, 487
Schmitz F., Steffens S., 1999, A&A 344, 973
Spruit H., 1977, Ph.D. Thesis, University of Utrecht
Stebbins R., Goode P., 1987, Solar Phys. 110, 237
Steffens S., 1998, Ph.D. Thesis, Universität Würzburg
Steffens S., Deubner F.L., Hofmann J., Fleck B., 1995, A&A 302, 277
Steffens S., Schmitz F., Deubner F.-L., 1997, Solar Phys. 172, 85
Ulrich R., Rhodes E., 1977, ApJ 218, 521
Vernazza J., Avrett E., Loeser R., 1981, ApJS 45, 635
Wolf B.E., 1983, A&A 127, 93